

# Semi-Automated Border Detection for Right Ventricular Volume Estimation from MR Images

Maria C Carminati<sup>1</sup>, Paola Gripari<sup>2</sup>, Francesco Maffessanti<sup>1,2</sup>, Cristiana Corsi<sup>3</sup>, Gianluca Pontone<sup>2</sup>, Daniele Andreini<sup>2</sup>, Mauro Pepi<sup>2</sup>, Enrico G Caiani<sup>1</sup>

<sup>1</sup>Politecnico di Milano, Biomedical Engineering Department, Milan, Italy

<sup>2</sup>Centro Cardiologico Monzino, IRCCS, Milan, Italy

<sup>3</sup>Università di Bologna, Bologna, Italy

## Abstract

*Two different methods for semi-automated right ventricular (RV) endocardial border detection from MR images, based on different implementation of level set technique, have been developed and validated.*

*Dynamic, ECG-gated, steady-state free precession short axis images were obtained in 26 consecutive patients. An expert cardiologist provided the “gold standard” for RV dimensions, by manually tracing the endocardial contours. Semi-automated detection was applied to obtain RV end-diastolic and end-systolic volumes, as well as stroke volume and ejection fraction.*

*Comparison with “gold standard” was performed by linear regression and Bland-Altman analyses. Results showed high correlations and small biases and narrow limits of agreement with the “gold standard” values. Both methods provided reliable measurements of RV dimensions; however, better accuracy is related to higher manual interaction.*

## 1. Introduction

Magnetic resonance (MR) imaging represents the gold standard for ventricular volumes and mass analysis. However, volumetric measurements are based on multiple contour tracing that makes the analysis cumbersome and subjective. While several semi-automated approaches exist to obtain left ventricular (LV) contours [1–3], very few have been tested and applied for right ventricular (RV) volume estimation [4]. Segmentation of cardiovascular MR images applied to RV endocardial detection is a challenging task: in fact, the RV cavity morphology is characterized by concavities and convexities, as well as the appearance of structures (chordae and papillary muscles) that could affect the contour detection performance. We hypothesized that segmentation algorithms based on level set technique [5], widely applied for LV contour detection, could be uti-

lized also for RV analysis.

Accordingly, our aim was to propose and validate against a manual gold standard two semi-automated methods, based on different implementations of level set technique, for RV endocardial detection applied to short axis MR images to determine RV volumes and function.

## 2. Methods

### 2.1. MR imaging

Dynamic, ECG-gated, steady-state free precession short axis images were acquired during breath hold (GE Healthcare, 1.5T) in 8–12 slices from the atrio-ventricular ring to the apex in 26 consecutive patients (20 or 30 phases/cardiac cycle, slice thickness 8 mm with no overlap and no gap). Informed consent was obtained from each patient.

### 2.2. Region-based level set

The first proposed approach for semi-automated RV endocardial contour detection is based on region-based (RB) image noise distribution followed by a variational level set formulation without re-initialization [6, 7]. The block diagram of the whole procedure is presented in figure 1.

The first part of the algorithm is based on a priori knowledge of the statistical distribution of gray levels in MR images, where image pixel videointensities are modelled as Gaussian distributed random variables. This method has been proposed and applied to LV endocardial segmentation [2, 3]. The initial surface evolves until the region probability terms of the inside region are equal to the terms of the outside region, thus driving the curve evolution to achieve a maximum-likelihood (ML) segmentation of the target, with respect to the statistical distribution law of pixel videointensity. First, a rectangular region of interest (ROI) including the RV is selected to avoid other structures to affect the performance of the ML segmentation method.

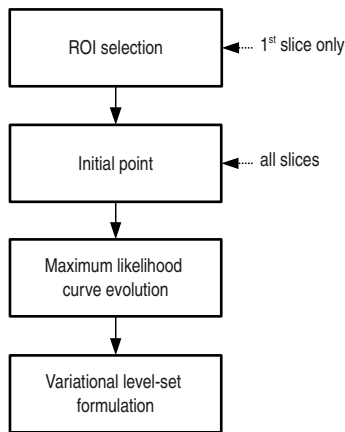


Figure 1: Block diagram of the region-based method.

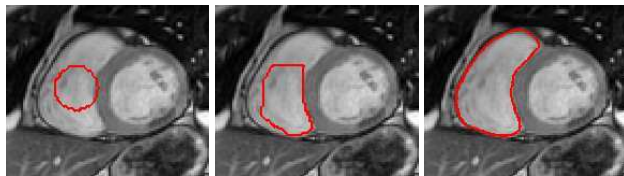


Figure 2: Region-based level set algorithm; first step: initialization 10 pixels radius circle (left panel); second step: ML segmentation (middle panel); last step: level set evolution based on variational formulation (right panel).

Then, a single point is selected inside the RV cavity and the initial contour is defined as a circle with center in the chosen pixel and radius of 10 pixels (figure 2, left panel). The result of this step alone (figure 2, center panel) is not satisfactory for RV endocardial detection due to the remarkable presence of chordae and papillary muscles that affect the ML process. Therefore, this partial result is used as initial condition for a following level set evolution based on a variational formulation without re-initialization (figure 2, right panel). This approach forces the level set function to be closed to a signed distance function, eliminating the need of the costly re-initialization procedure and allowing to use a significantly larger time step for numerically solving the evolution of the partial differential equation, speeding up the process.

### 2.3. Edge-based level set

The second method for endocardial RV detection is based on edge-based (EB) image gradient level set method followed by a regularization procedure based on curvature motion [5, 8]. To overcome limitations of the level set approach due to the RV morphology, strongly characterized

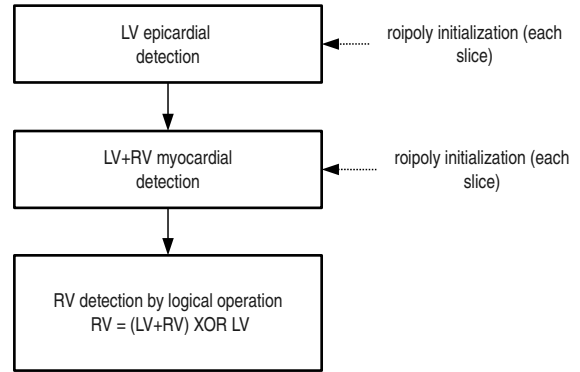


Figure 3: Block diagram of the edge-based method.

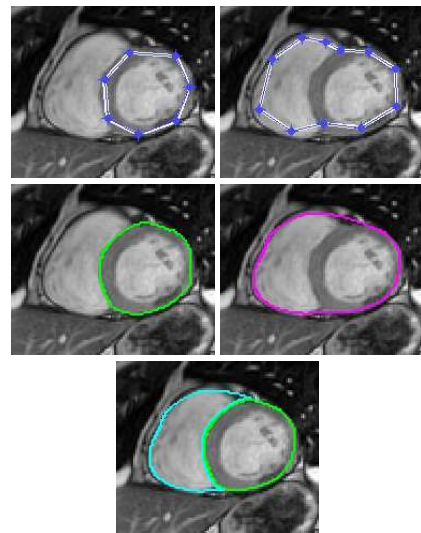


Figure 4: Edge-based level set algorithm; top row: polygonal initialization of LV and (RV+LV); middle row: results of level set evolution; bottom row: RV segmentation result as LV XOR (RV+LV).

by concavities and convexities with angular points, and inhomogeneous RV cavity videointensity, our idea was to obtain the RV endocardial contour by first detecting joint myocardial RV and LV contours (RV+LV) and then subtracting the LV epicardial contour (figure 3).

For each slice and for each (RV+LV) and LV contours an initialization representing the vertexes of a polygon was provided by the user and used as initial contour for the level set algorithm. The final RV contour was obtained by logical XOR operation between the (RV+LV) contour and the LV epicardial contour (figure 4).

## 2.4. RV volume quantification

For both methods, after RV endocardial border detection, EDV and ESV were computed by disk-area summation method, measuring areas in each slice as pixel counts inside the contour and multiplying by the pixel spatial resolution and slice thickness, obtained from the DICOM header. EDV and ESV were then used to compute stroke volume (SV) and ejection fraction (EF).

## 2.5. Validation with the “gold standard”

Cardiac MR images were analyzed using commercial software (MASS 6.1, Medis, Leiden, Netherlands) installed on the MR workstation. An expert cardiologist proceeded into the conventional analysis of these images, by manually tracing the RV endocardial contours. Then, RV end-diastolic (EDV) and end-systolic (ESV) volumes were measured using standard volumetric techniques, and SV and EF derived. Linear correlation and Bland-Altman (applied as ratio between the tested methods and the gold standard, to eliminate for potential linear correlation of the bias with the RV size) analyses were applied to evaluate the accuracy of each of the two semi-automated techniques.

## 3. Results

The analysis with the RB method was feasible in 24/26 (92%) patients; in the remaining two patients the significant presence of chordae and papillary muscles prevented a satisfactory performance. Conversely, feasibility of the analysis with the EB method was 100%.

Both methods were developed in Matlab (The Mathworks Inc, Natick, Massachusetts) using a 64-bits GNU/Linux environment (quad-core Q8400 CPU, 4 Gb of DDR3 RAM) and the time required to process a single frame (all slices) was approximately 2-3 min. The performance of the RB method depended on the position of the selected initial point, thus multiple trial-and-test initialization was often required to obtain visually acceptable final contours.

For both the proposed methods, good correlation was found against the gold standard measurements. In particular, the RB method resulted in the following: EDV:  $y = 0.89x + 2.39$ ,  $r^2 = 0.88$ ; ESV:  $y = 0.75x + 9.887$ ,  $r^2 = 0.85$ ; SV:  $y = 1.08x - 2.73$ ,  $r^2 = 0.77$ ; EF:  $y = 1.02x - 2.73$ ,  $r^2 = 0.65$ . The EB method resulted in: EDV:  $y = 1.11x - 6.92$ ,  $r^2 = 0.91$ ; ESV:  $y = 1.25x + 4.63$ ,  $r^2 = 0.92$ ; SV:  $y = 0.94x - 5.63$ ,  $r^2 = 0.69$ ; EF:  $y = 0.99x - 10.9$ ,  $r^2 = 0.71$ . Results of Bland-Altman analysis are shown in table 1 (RB method) and 2 (EB method), where negative bias means underestimation in respect of the gold standard. The RB method significantly underestimated RV EDV, while the EB method

Table 1: Results of the Bland-Altman analysis for the region-based method (\*:  $p < 0.05$  paired t-test vs null).

	region-based method	
	bias	95% limits of agreement
EDV (ml)	-12*	-40 ÷ 16
ESV (ml)	-3	-21 ÷ 15
SV (ml)	-9*	-35 ÷ 17
EF (%)	-2	-18 ÷ 14

Table 2: Results of the Bland-Altman analysis for the edge-based method (\*:  $p < 0.05$  paired t-test vs null).

	edge-based method	
	bias	95% limits of agreement
EDV (ml)	8 *	-20 ÷ 36
ESV (ml)	20 *	-2 ÷ 42
SV (ml)	-11*	-36 ÷ 14
EF (%)	-11*	-24 ÷ 2

significantly overestimated both EDV and ESV. The RB method showed a narrower limits of agreement in ESV, while the one for EDV was similar. Both methods underestimated SV of about 10 ml, resulting in an underestimation of EF for the EB method, but with narrower limits of agreement. Figure 5 shows correlation and Bland-Altman analyses for the two methods separately, but considering EDV and ESV measures all together (bias $\pm$ 2SD, RB method:  $-9 \pm 32$  ml, EB method:  $24 \pm 32$  ml ).

## 4. Discussion and conclusions

We have presented two methods for semi-automated RV endocardial detection from MR short axis images with the aim to reduce manual interaction in the assessment of RV volumes and function.

Statistical analysis showed that both methods provided good agreement with the gold standard. However, RB tended to underestimate RV volume while EB tended to overestimate it. This can be explained by the fact that in the RB method internal parts of the RV close to the LV junctions, similar to angular points, remain outside the detected contour. Conversely, in the EB method these points are always included, but together with additional pixels outside the RV chamber due to the curvature motion of the regularization process in the (RV+LV) segmentation.

With both methods, computed limits of agreement were similar but their width, hence narrow, could suggest a careful clinical interpretation of the results, depending of the population under study.

As regards user interaction, with the RB method the ini-

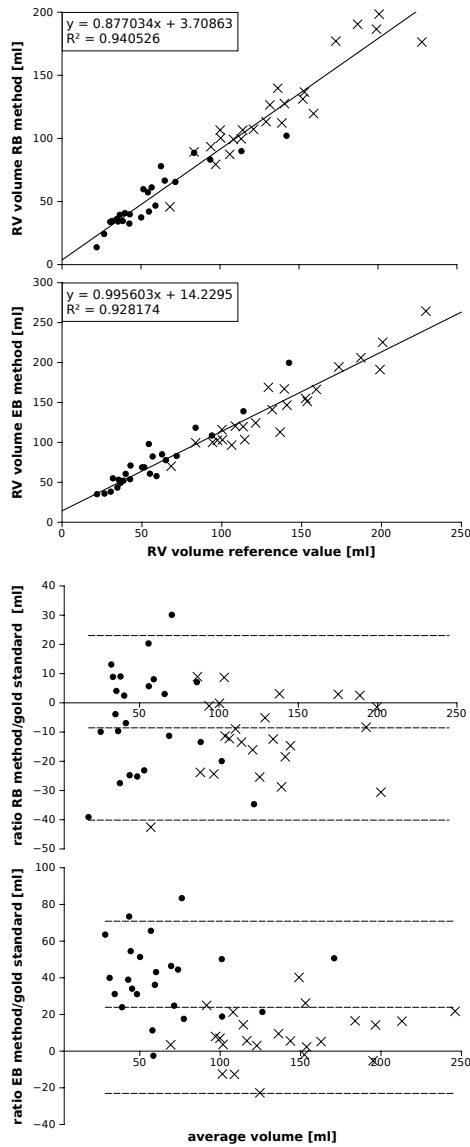


Figure 5: Correlation and Bland-Altman analyses for RB, 1<sup>st</sup> and 3<sup>rd</sup> panel, and EB methods, 2<sup>nd</sup> and 4<sup>th</sup> panel (×: ED values, •: ES values).

tialization process is potentially minimized since only one point has to be selected in each slice. However, due to the presence of cordae and papillary muscles which result in marked inhomogeneity of the RV cavity videointensity, the front evolution of the level set can be influenced by the position of the initialization point. In fact, in about 50% of the analyzed patients, multiple (up to three) trial-and-test initializations were needed to obtain visually acceptable contours. On the contrary, the EB method required higher user interaction with two separate initializations of

polygonal contours. However, there was no need to repeat this process as the initial conditions were less dependent on the structures in the RV cavity.

In conclusion, our results showed that both the proposed methods provide reliable measurements of RV dimension and function. However, better accuracy is related to higher manual interaction. Further improvements, like pre-processing of the RV chamber to reduce papillary muscle-related artifacts, need to be explored to solve this limitation.

## References

- [1] Paragios N. A level set approach for shape-driven segmentation and tracking of the left ventricle. *Medical Imaging IEEE Transactions on* 2003;22(6):773–776.
- [2] Corsi C, Veronesi F, Lamberti C, Bardo D, Jamison E, Lang R, Mor-Avi V. Automated frame-by-frame endocardial border detection from cardiac magnetic resonance images for quantitative assessment of left ventricular function: Validation and clinical feasibility. *Journal of Magnetic Resonance Imaging* 2009;29(3):560–568.
- [3] Conti C, Votta E, Corsi C, De Marchi D, Tarroni G, Stevanella M, Lombardi M, Parodi O, Caiani E, Redaelli A. Left ventricular modelling: a quantitative functional assessment tool based on cardiac magnetic resonance imaging. *Interface Focus* 2011;1(3):384–395.
- [4] Lemmo M, Azarine A, Tarroni G, Corsi C, Lamberti C. Estimation of right ventricular volume, quantitative assessment of wall motion and trabeculae mass in arrhythmogenic right ventricular dysplasia. In *Computers in Cardiology*, 2010, volume 37. IEEE; 805–808.
- [5] Malladi R, Sethian J, Vemuri B. Shape modeling with front propagation: A level set approach. *Pattern Analysis and Machine Intelligence IEEE Transactions on* 1995;17(2):158–175.
- [6] Gravel P, Beaudoin G, De Guise J. A method for modeling noise in medical images. *Medical Imaging IEEE Transactions on* 2004;23(10):1221–1232.
- [7] Li C, Xu C, Gui C, Fox MD. Level set evolution without re-initialization: A new variational formulation. *Computer Vision and Pattern Recognition IEEE Computer Society Conference on* 2005;1:430–436. ISSN 1063-6919.
- [8] Malladi R, Sethian J. Image processing via level set curvature flow. *Proceedings of the National Academy of sciences* 1995;92(15):7046–7050.

Address for correspondence:

Maria Chiara Carminati  
 Politecnico di Milano, Biomedical Engineering Dpt  
 Piazza L. da Vinci 32, 20133 Milan, Italy  
 maria.carminati@mail.polimi.it